Available online at www.sciencedirect.com

SciVerse ScienceDirect

Ceramics International 39 (2013) 81–86

CERAMICS INTERNATIONAL

www.elsevier.com/locate/ceramint

MCMB–SiC composites; new class high-temperature structural materials for aerospace applications

Saeed Safi, Asghar Kazemzadeh*

Ceramic Department, Materials and Energy Research Center, Karaj, Iran

Received 25 June 2011; received in revised form 24 May 2012; accepted 30 May 2012
Available online 7 June 2012

Abstract

Graphite–silicon carbide (G–SiC), carbon/carbon–silicon carbide (C/C–SiC) and mesocarbon microbeads–silicon carbide (MCMB–SiC) composites were produced using liquid silicon infiltration (LSI) method and their physical and mechanical properties, including density, porosity, flexural strength and ablation resistance were investigated. In comparison with G–SiC and C/C–SiC composites, MCMB–SiC composites have the highest bending strength (210 MPa) and ablation resistance (9.1%). Moreover, scanning electron microscopy (SEM) and optical microscopy (OM) are used to analyze the reacted microstructure, pore morphology and pore distribution of carbon-based matrices. As a result, SiC network reinforcement was formed in situ via a reaction between liquid silicon and carbon. The unreacted carbon and solidified silicon are two phases present in the final microstructure and are characterized by X-ray diffraction (XRD). Based on the results obtained and the low-cost processing of pitch-based materials, the MCMB–SiC composite is a promising candidate for aerospace applications.

Keywords: Mesocarbon microbeads; Liquid silicon infiltration; CMC; SiC reinforcement

1. Introduction

Thanks to their low density, high thermal conductivity, low thermal expansion and good tribological behavior ceramic matrix composites (CMCs) are considered a new class of engineering materials in aerospace structures [1]. These composites are generally made by three different techniques: chemical vapor infiltration (CVI), liquid polymer infiltration (LPI) and liquid silicon infiltration (LSI). This last technique is of great interest to the ceramist for its low cost, manufacturing simplicity, short processing time, cheap raw materials and near net shape susceptibility. Brake and clutch disks, heat exchangers, calibration plates, mirror of space telescopes and furnace-charging equipment are engineering parts that can be produced using LSI method [2–5]. The LSI process involves two main stages: first, porous carbon performs are fabricated and then siliconization is performed. During the siliconization process, the crack pattern of carbon body, capillary effect of the open pores and low viscosity of molten silicon enable formation of SiC network reinforcement on the carbon–silicon interface [6,7]. As one of the mesophase carbon material, mesocarbon microbeads (MCMB) have many excellent properties, such as self-sinter at low temperatures, chemical inertness, high packing density, planar carbon layer structure and are used for manufacturing high strength and high-density carbon materials [8–11]. These materials are extracted from the mesophase pitch and contain oligomers, with aromatic planes that are nearly parallel and arranged in one direction [12]. This special structure is the origin of advanced properties of the MCMBs such as self-sintering capability, homogeneous contraction, high-carbon residues and easy graphitization. At present, these materials are under investigation for use in various fields: pistons for combustion engines, battery anodes and mechanical seals [13–16]. The goal of this work is to use MCMBs, carbon-based fabric PAN and graphite as porous carbon substrates to prepare reaction-bonded carbon–SiC composites. For this purpose, these matrices

*Corresponding author.
E-mail address: a-kazemzadeh@merc.ac.ir (A. Kazemzadeh).

0272-8842/$36.00
http://dx.doi.org/10.1016/j.ceramint.2012.05.098

were preformed and then SiC-reinforced composites were prepared using the liquid silicon infiltration method. The microstructure, phase composition and properties of prepared composites were investigated.

2. Experimental procedure

2.1. Carbon-porous body

2.1.1. Graphite-porous body

Graphite powder with less than 0.1% ash and 30–50 mesh of particle size was prepared as filler and the phenolic resin (see Table 1) was used as binder. To produce porous graphite preform, first the phenolic resin was dissolved in ethanol to prepare a precursor solution with a molar ratio of resin:ethanol of 1:1. The graphite powder was then added to the above solution. The ethanol was evaporated by continuous mixing during heating at 100 °C on a warm mixer. The dried precursor was cold isostatically pressed (CIPed at 100 MPa) into pellets of 10 cm diameter which were then heat-treated in nitrogen atmosphere (heating rate: 0.5 °C/min) in a box furnace at 1000 °C. The physical and mechanical properties of graphite matrix are shown in Table 5.

2.1.2. Carbon–carbon porous body

A vacuum-bagging technique plus a hot press (30 bar, 160 °C) were employed to prepare porous C/C preform. In this method, several layers of two-dimensional plain woven carbon-based fabric PAN were stacked up inside the chamber of the mold. The polymer phenolic resin was allowed to enter the system from one end while keeping the vacuum pump running at another end. Carbonization of the as-cured composite plate was performed at 1000 °C under a nitrogen atmosphere (heating rate: 0.5 °C/min). The profile of polymer phenolic resin and properties of C/C matrix are shown in Tables 2 and 5 respectively.

2.1.3. MCMB-porous body

It is known that the properties of polyaromatic mesophases depend on the manufacturing extraction and pretreatment procedures [17]. We have used one type of commercially available MCMB (Osaka Gas, Japan), whose characteristics are shown in Table 3. Before heat treatment at a high temperature, the MCMB was calcined at 373 K in the air for 12 h. It was qualitatively observed that such a process causes a mild oxidation of the MCMB which improves the final sample quality [18]. After this process, the MCMB materials were CIPed under different pressures (50,100, 150, 200 MPa). The green performs were then carbonized in nitrogen atmosphere (heating rate: 0.5 °C/min) in a box furnace heated to 1000 °C. The results show that the porosity of the sample CIPed at 50 MPa pressure is comparable to the porosity of graphite and C/C performs. Hence it was selected for the siliconization process. The mechanical and physical properties of these three types of carbon preforms are compared in Table 5.

Table 1
The phenolic resin profile.

Free phenol (%)	Hexsamine (%)	Melting range (°C)	B.time (150 °C) s
Max 1%	9 ± 1	85–110	80–100

Table 2
Carbon-based fabric pan profile.

Tensile modulus (GPa)	Tensile strength (MPa)	Surface density (g/m^2)	Carbon fabric
230	3450	320 ± 5	PAN-T300-6K

2.2. Siliconization

Siliconization of the porous samples was performed in a high-temperature vacuum electric furnace heated to 1450 °C under a residual pressure of 10^{-3} mbar. The profile of the silicon used in this study is shown in Table 4. The processes flow charts for production of C/C–SiC, G–SiC and MCMB–SiC composites via liquid silicon infiltration are shown in Fig. 1.

2.3. Characterization

Reaction-bonded carbon–SiC (RBSC) specimens were cut by a diamond blade and then mounted in epoxy resin and polished to the mirror-surface condition for microscopic investigations. The density and open porosity of preforms and reacted microstructure were measured using Archimedes' method to the ASTM standard C830-91 method. To evaluate the flexural strength before and after siliconization process, the four-point-bending test, according to the ASTM standard C1341-97, was used. The phases of the composites were characterized by X-ray diffraction (XRD) (Philips pw3710 with Cu Kα radiation, $\lambda = 0.15406$ nm). To evaluate the oxidation resistance and ablation performance of the composites, the oxyacetylene standard flame test was carried out

Table 3
MCMB profile.

Particle size (μm)	10% < 0.66 50% < 5.34 90% < 14.22
%TI	95.6
%QI	91.2
%β-Resin	4.4

Table 4
Chemical analysis of silicon.

%Ca	%K	%Fe	%Al	%Si
0.3	0.21	0.21	0.53	98.75

according to ASTM-E-285–80. This test can create hot gas with 3000 K and 8×10^6 W m^{-1} K^{-1} heat flux [19]. The temperature of the oxyacetylene flame was measured using a laser pyrometer. Fig. 2 shows the oxyacetylene ablation facility operating at approximately 2000 °C. The samples were exposed to hot combustion gases for 30 s and then the changes in weight and dimensions were measured.

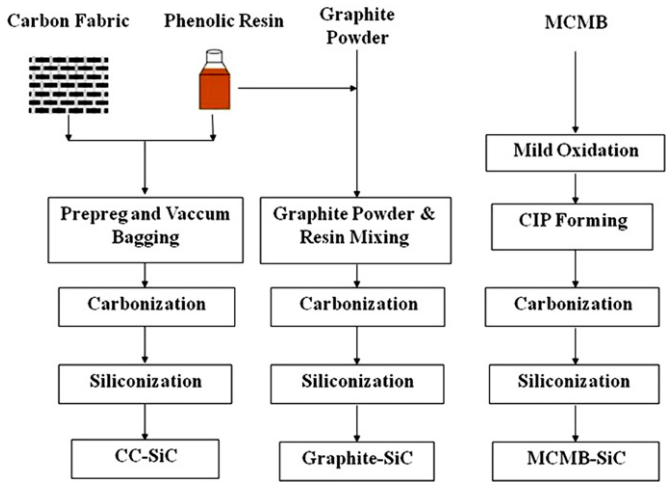

Fig. 1. Process flow chart for production of C/C–SiC, G–SiC and MCMB–SiC composites using liquid silicon infiltration method.

3. Results and discussion

3.1. Properties of carbon preforms and reaction-bonded C–SiC composites

Table 5 lists the densities, porosities and bending strengths of preforms and SiC-reinforced composites. The MCMB preform has the lowest porosity (15°), while the graphite body has the highest amount of open porosity (19.5%). Investigations show that the pore structure is formed in the carbonization of the carbon body [4]. The presence of porosity in carbon preform can be attributed to the binder contraction, gas release, microstructural transformation and carbonization of constituents such as β-resin [10]. In the liquid silicon infiltration method, molten silicon is infiltrated into the preforms and reacted with carbon to form SiC reinforced composite. The in-situ formed SiC and some unreacted silicon replaced the pores in the carbon matrix, resulting in higher densities of the composites (see Table 5). As a result, for the subsequent siliconization process and formation of the SiC reinforcement, the pore structure formed in the carbonization of preforms is of decisive importance, using only a suitable pore structure it can be ensured that liquid silicon will infiltrate uniformly into the body. The results show that MCMB–SiC composite has the minimum amount of open porosity (0.62%) and its bending strength showing the maximum value (210 MPa) demonstrated that MCMB preform with excellent sphericity creates a suitable pore structure for completion of LSI process.

Fig. 2. Oxyacetylene ablation facility operating at approximately 2000 °C.

Table 5
Measured specifications of composites before and after siliconization and ablation rate of composites.

Samples	Before siliconization			After siliconization			
	Density (g/cm^3)	Open porosity (%)	Bending strength (MPa)	Density (g/cm^3)	Open porosity (%)	Bending strength (MPa)	Mass ablation rate (g/s)
Graphite	1.50	19.5	24	2.40	1.41	50	2.635
Carbon–carbon	1.45	18	27	2.21	2.10	120	2.153
MCMB	1.50	15	30	2.41	0.62	210	1.837

3.2. XRD patterns of G–SiC and MCMB–SiC composites

XRD patterns of the siliconized products for G–SiC and MCMB–SiC are shown in Fig. 3. For MCMB–SiC composite, peaks assigned to SiC and very small peaks corresponding to residual Si and unreacted carbon are clearly observed in Fig. 3(a). But for G–SiC, the intensity of SiC peaks decreased and the intensity of carbon and Si increased, as shown in Fig. 3(b). It meant that reactivity of graphite at siliconization temperature is smaller than in MCMB.

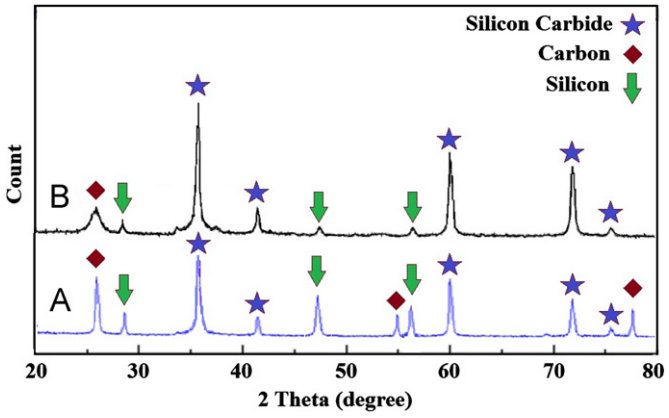

Fig. 3. XRD patterns of reaction-bonded composites: (a) G–SiC and (b) MCMB–SiC.

3.3. Microstructure of the SiC-reinforced composites

SEM and OM micrographs of the graphite preform and polished cross-sections of the G–SiC composite are shown in Fig. 4. The graphite porous preform has a weak spongy microstructure. For G–SiC, the light brown, black and white regions in the images are identified as silicon carbide, carbon and silicon respectively (see Fig. 4(C) and (D)). It can be seen that the volume fractions of unreacted carbon and Si are noticeable. Fig. 5 shows the microstructure of the C/C–SiC composite after the siliconization process. The micrographs show the dark region of C/C segments, gray region of SiC and white region of unreacted Si. From the enlarged SEM image of Fig. 5 (B) taken from the region marked 'I', it is clear that the liquid silicon successfully infiltrated into the microchannels and into SiC formed at the interface of C/C segments and liquid silicon. The cross-sectional and polished OM and SEM micrographs of MCMB–SiC composite are shown in Fig. 6. The microstructure analysis revealed that there was less residual carbon but more SiC produced due to high reactivity of the MCMB preform.

3.4. Ablation rate of composite

The ablation rate of MCMB–SiC, C/C–SiC and G–SiC composites are also presented in Table 5. It can be easily seen that the ablation rate of MCMB–SiC was much lower

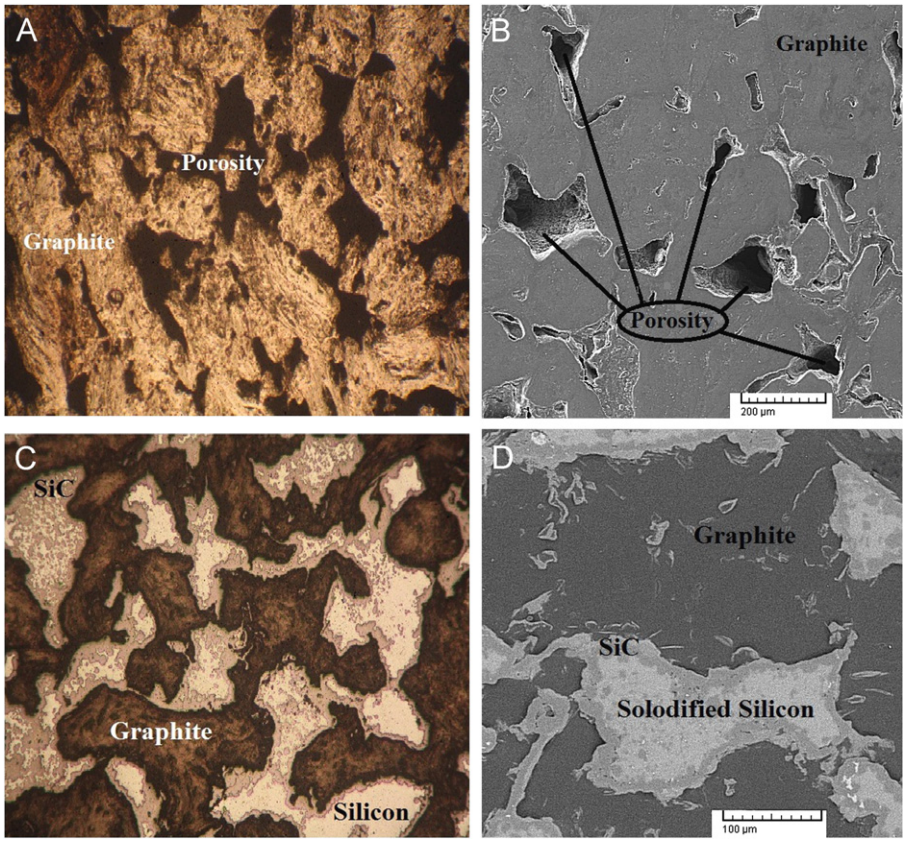

Fig. 4. OM and SEM micrographs of graphite preform and G–SiC composite. (A) and (B) Graphite preform (C) and (D) G–SiC composite.

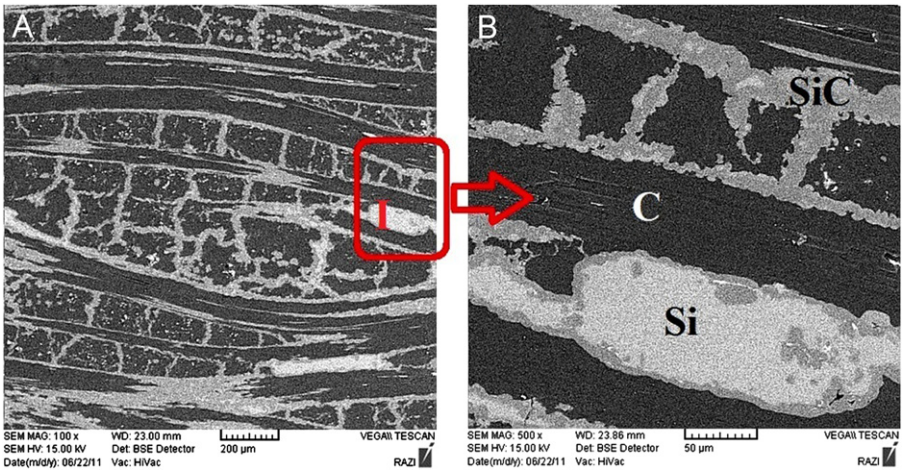

Fig. 5. SEM micrographs of C/C–SiC Composite (A) C/C segments (dark), SiC (gray) and Si (white) and (B) enlarged image marked 'I'.

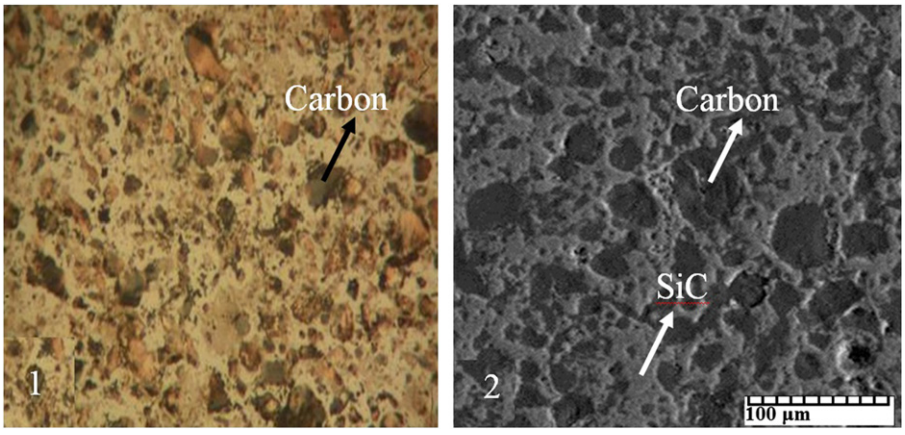

Fig. 6. Micrographs of MCMB–SiC composite. (1) Optical micrograph and (2) SEM micrograph.

than that in other two composites. The oxidation erosion and mechanical denudation are two kinds of the important ablation mechanism which explain the ablation properties of reaction-bonded carbon–SiC composites [20]. As the oxyacetylene flame reaches the surface of the composites, the temperature of the composites will rapidly increase and oxidation gases will react with SiC, Si and carbon [20]. SiC and Si are two vulnerable phases and will be oxidized into SiO in gas form directly. Compared with other carbon matrices, MCMB plays an important role in the ablation resistance of MCMB–SiC composite. Since MCMB preform prepares a suitable pore structure, liquid silicon can be infiltrated uniformly and in sufficient amount into the body. Homogeneous dispersion of in situ formed SiC as a reinforced phase into the carbon matrix and the reduced amount of unreacted Si phase are two advantages of MCMB matrix.

4. Conclusions

MCMB–SiC, C/C–SiC and G–SiC were fabricated by infiltrating molten Si into the carbon matrices. The MCMB–SiC composite has the minimum amount of open porosity (0.62%) and its bending strength showing the maximum value (210 MPa) demonstrated that MCMB preform with excellent sphericity creates a suitable pore structure for completion of the LSI process. The ablation resistance of MCMB–SiC was much lower than that of the other two composites. Homogeneous dispersion of in-situ formed SiC as a reinforced phase into the carbon matrix and the reduced amount of unreacted Si phase are two advantages of MCMB matrix. Based on the results obtained and the low-cost processing of pitch-based materials, the MCMB–SiC composite is a promising candidate for aerospace applications.

Acknowledgements

The authors thank Yousef Safaei-Naeini and Iman Najafi-Hajivar for discussions assistance. The authors also acknowledge Fatemeh Khorasanizadeh for her technical support.

References

[1] B. Heidenreich, Melt infiltration, in: W. Krenkel (Ed.), Ceramic Matrix Composites: Fiber Reinforced Ceramics and their Applications, WILEY-VCH Verlag GmbH & Co, New York, 2008, pp. 113–140.

[2] M. Singh, D.R. Behrendt, Microstructure and mechanical properties of reaction-formed silicon carbide (RFSC) ceramics, Materials Science and Engineering: A 187 (1994) 183–187.

[3] Y.M. Chiang, R.P. Messner, C.D. Terwilliger, D.R. Behrendt, Reaction-formed silicon carbide, Materials Science and Engineering: A 144 (1991) 63–74.

[4] N.R. Calderon, M. Martínez-Escandell, J. Narciso, F. Rodríguez-Reinoso, The combined effect of porosity and reactivity of the carbon preforms on the properties of SiC produced by reactive infiltration with liquid Si, Carbon 47 (2009) 2200–2210.

[5] M. Singh, D.R. Behrendt, Reactive melt infiltration of silicon-molybdenum alloys into microporous carbon performs, Materials Science and Engineering: A 194 (1995) 193–200.

[6] B. Heidenreich, R. Renz, W. Krenkel, Short fiber reinforced CMC materials for high performance brakes, in: W. Krenkel (Ed.), High Temperature Ceramic Matrix Composites, New York, 2001, pp. 809–815.

[7] K. Rebelo, M. Hofmann, Non-desting of satellite nozzles made of carbon fibre ceramic matrix composite, C/SiC, Materials Characterization 58 (2007) 922–927.

[8] I. Mochida, R. Fujiura, T. Kojima, H. Sakamoto, T. Yoshimura, Carbon disc of high density and strength prepared from heat-treated mesophase pitch grains, Carbon 33 (1995) 265–274.

[9] Y.G. Wang, Y. Korai, I. Mochida, Carbon disc of high density and strength prepared from synthetic pitch-derived mesocarbon microbeads, Carbon 37 (1999) 1049–1057.

[10] C. Norfolk, A. Mukasyan, D. Hayes, P. McGinn, A. Varma, Processing of mesocarbon microbeads to high-performance materials: part I. Studies towards the sintering mechanism, Carbon 42 (2004) 11–19.

[11] L. Tongqi, C. Wang, L. Xiujun, J. Zheng, W. Hui, SEM analysis of the changes of carbon layer structure of mesocarbon microbeads heat-treated at different temperature, Chinese Science Bulletin 49 (2004) 1105–1110.

[12] I. Mochida, Y. Korai, C.H. Ku, F. Watanabe, Y. Sakai, Chemistry of synthesis, structure, preparation and application of aromatic-derived mesophase pitch, Carbon 38 (2008) 305–308.

[13] Y. Song, G. Zhai, G. Li, J. Shi, Q. Guo, L. Liu, Carbon/graphite seal materials prepared from mesocarbon microbeads, Carbon 42 (2004) 1427–1433.

[14] G. Bhatia, R.K. Aggarwal, N. Punjabi, O.P. Bahl, Effect of sintering temperature on the characteristics of carbons based on mesocarbon microbeads, Journal of Materials Science 32 (1997) 135–139.

[15] J. Schmidt, K.D. Moergenthaler, K.P. Brehler, J. Arndt, High-strength graphites for carbon piston applications, Carbon 36 (1998) 1079–1084.

[16] M.H. Chen, G.T. Wu, G.M. Zhu, Characterization and electrochemical investigation of boron-doped mesocarbon microbead anode materials for Li-ion batteries, Journal of Solid State Electrochemistry 6 (2002) 420–427.

[17] C. Norfolk, A. Mukasyan, D. Hayes, P. McGinn, A. Varma, Processing of mesocarbon microbeads to high-performance materials: part II. Reaction bonding by in situ silicon carbide and nitride, Carbon 44 (2006) 293–300.

[18] C. Norfolk, A. Mukasyan, D. Hayes, P. McGinn, A. Varma, Processing of mesocarbon microbeads to high-performance materials: part III. High temperature sintering and graphitization, Carbon 44 (2006) 301–306.

[19] A.R. Bahramian, M. Kokabi, M.H.N. Famili, M.H. Beheshti, Ablation and thermal degradation behavior of a composite based on a resol type phenolic resin: process modeling and experimental, Polymer 47 (2006) 3661–3673.

[20] J. Yin, H. Zhang, X. Xiong, J. Zuo, H. Tao, Ablation properties of C/C–SiC composites tested on an arc heater, Solid State Sciences 13 (2011) 2055–2059.